Modeling Heat Mitigation in Hollow-Core Gas Fiber Lasers With Gas Flow

Wei Zhang, *Graduate Student Member, IEEE*, Ryan A. Lane, Curtis R. Menyuk, *Life Fellow, IEEE*, and Jonathan Hu, *Senior Member, IEEE*

(Invited Paper)

***Abstract*—We carry out a computational study to evaluate the temperature reduction by using gas flow in hollow-core gas fiber lasers. We first use the Navier-Stokes equations to study the gas flow in the hollow-core fibers. We compare the density, pressure, and velocity using both an incompressible and a compressible gas model. We show that an incompressible gas model leads to large errors in the case that we study in this paper. We then present a coupled model to study gas flow and heat transfer simultaneously in hollow-core fibers using a compressible gas model. We found that a temperature reduction of about 20% can be achieved by using a differential pressure of 10 atm between the inlet and outlet of the hollow-core fibers. The results also demonstrate that the relative temperature reduction increases when the heat power decreases, the fiber length decreases, and the heat profile is more localized.**

***Index Terms*—Hollow-core fiber lasers, compressible gas flow, thermal dynamics, heat mitigation.**

I. Introduction

GAS lasers have been studied extensively over the years for applications in sensing, medical, and defense fields [1], [2]. Gas lasers have larger damage thresholds compared to step-index fiber lasers since the light propagates in a gas core rather than a glass core. Compared with rare-earth-doped fiber lasers, gas lasers can lase at higher power levels due to the weaker nonlinearity of the gas medium. While step-index fiber lasers can have impressive powers on the order of kilowatts, gas lasers can reach megawatts [3]. The invention of hollow-core fibers enables new gas-filled hollow-core fiber lasers and sensors [4], due to their ability to host gases for long interaction lengths and the micrometer-scale mode areas in the hollow-core fiber [5], [6], [7], [8]. Gas-filled hollow-core fibers are attracting much attention as they have remarkable linear and nonlinear properties and have been used in several critical applications including gas lasers, high-power fiber delivery, pulse shaping, and nonlinear optics. The high optical intensity that can be obtained in hollow-core fibers enables the study of the nonlinear interaction of light with gases, vapors, and plasmas—all of which can be introduced into the hollow core. Early work on nonlinear optics in hollow-core fibers used bandgap or kagome fibers [5], [9], [10], [11]. More recent work uses negative curvature fibers [12], [13], [14] due to their low loss. The small overlap between the guided optical field and cladding glass, which is on the order of 10^{-5}, leads to a significant increase in the damage threshold beyond what is possible in hollow-core bandgap fibers [12], [13], [14]. The fabrication technology has become mature with the introduction of commercial products. The relative simplicity of the negative curvature structure facilitates the fabrication of fiber devices using non-silica glasses, such as chalcogenide [15], [16]. Since the gas media can be easily changed, gas-filled hollow-core fiber lasers can lase over a wide range of emission wavelengths from UV to IR.

Due to the high output power obtained in gas fiber lasers, heat has become a major factor in limiting the output power from gas laser systems. In order to achieve high output power, it is essential to reduce the temperature in the optical fiber. Consequently, there is a critical need to study the heat dissipation in gas-filled hollow-core fibers to determine the maximum output power at which gas lasers can operate. It is a unique feature of hollow-core fibers that gas flow [17], [18], [19] can be used to decrease the temperature. In this paper, we will theoretically evaluate the thermal mitigation that can be achieved by using gas flow. Numerical models based on the Navier–Stokes equations can be used to study pressure-driven gas flow in hollow-core fibers and provide helpful information such as the velocity profile. Many studies solve the Navier-Stokes equations using the assumption that the gas is incompressible [20], [21], [22], [23]. In this work, we will extend our earlier work [24] and describe a detailed study of gas flow within hollow-core fibers, comparing models where the gas is treated as either compressible or incompressible. We found that the use of an incompressible model is inadequate, and it is necessary to use a compressible model. In addition, we study gas flow and heat transfer simultaneously in gas-filled hollow-core fibers. The purpose of this study is to determine the temperature reduction due to gas flow that is driven by pressurized gas at the fiber input. We propose a coupled model to study gas flow and heat transfer, as gas flow will increase the heat dissipation, and temperature variation will change the gas density in the gas-filled hollow-core

Manuscript received 10 April 2024; revised 3 June 2024 and 5 July 2024; accepted 8 July 2024. Date of current version 2 August 2024. *(Corresponding author: Jonathan Hu.)*

Wei Zhang and Jonathan Hu are with the Baylor University, Waco, TX 76798 USA (e-mail: wei_zhang3@baylor.edu; jonathan_hu@baylor.edu).

Ryan A. Lane is with the Air Force Research Laboratory, Kirtland, NM 87117 USA (e-mail: ryan.lane.5.ctr@us.af.mil).

Curtis R. Menyuk is with the University of Maryland Baltimore County, Baltimore, MD 21250 USA (e-mail: menyuk@umbc.edu).

Color versions of one or more figures in this article are available at https://doi.org/10.1109/JSTQE.2024.3430929.

Digital Object Identifier 10.1109/JSTQE.2024.3430929

fiber. We use an iterative approach to find a self-consistent stationary solution, given the heat as a function of position in the fiber.

The heat profile that is generated in hollow-core gas-filled fiber lasers is unknown. Simple estimates of the heat power that may be found in the literature vary over a wide range, spanning 1 mW to 50 W [25], [26], [27], [28], [29]. Our goal is to demonstrate that a significant temperature reduction can be obtained almost regardless of the heat profile and the total heat power, and for that reason we consider a range of heat powers and profiles, as well as fiber lengths and input pressures. Our studies reveal that at the maximum differential pressure that we considered (10 atm) and with a heat power of 5 W the reduction can be as high as 20%.

The remainder of this paper is organized as follows: In Section II, we present a gas flow model in hollow-core fibers based on the Navier–Stokes equations. We analyze the results of our gas flow model, comparing the gas flow model assuming incompressible or compressible gas. In Section III, we explain the coupled model to study gas flow and heat transfer simultaneously. In Section IV, we show the temperature mitigation achieved through gas flow in hollow-core fibers for various conditions. Finally, we conclude in Section V.

II. Gas Flow Model

We first study the gas flow model. Gas is introduced into the hollow-core fiber with a high pressure at the inlet. The gas encounters ambient pressure at the outlet. The motion of the gas is described by the Navier-Stokes equations [30], [31], [32]. The momentum equation in steady state may be written as

$$\rho \left(\mathbf{u} \cdot \nabla\right) \mathbf{u} = \nabla \cdot \mathsf{K} - \nabla p, \tag{1}$$

where $\mathbf{u}$ is the fluid velocity, ρ is the density of the fluid, p is the pressure within the fluid, and K is viscous stress tensor. The viscous stress in turn may be written $\mathsf{K} = \mu(\nabla\mathbf{u} + \nabla\mathbf{u}^T) - 2\mu(\nabla \cdot \mathbf{u})\mathrm{I}/3$, where I is the identity matrix and μ is the viscosity of the fluid. The gas density is calculated using the ideal gas law so that $\rho = pM/(RT)$, where M is molar mass, R is the ideal gas constant, and T is temperature. Several prior studies of gas-filled fiber lasers solve the Navier-Stokes equations using the assumption that the gas is incompressible [20], [21], [22], [23]. In this paper, we will examine this assumption by comparing the results when we assume that the gas is incompressible and when it is compressible. For compressible flows, the continuity equation is written $\nabla \cdot (\rho\mathbf{u}) = 0$. By contrast, for incompressible flow, the continuity equation becomes $\nabla \cdot \mathbf{u} = 0$ since the density becomes constant. The primary goal of this paper is to explore the impact of temperature changes rather than to quantify flow characteristics precisely, and a simplified laminar flow model is assumed in this work, which provides valuable insights while maintaining a balance between accuracy and computational efficiency.

We solve the Navier-Stokes equations utilizing the commercially available simulation software, COMSOL Multiphysics. We will simplify the geometry using a simple cylindrical shape,

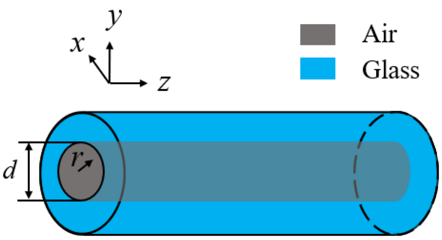

Fig. 1. Schematic illustration of the hollow core fiber, where *r* denotes the radial distance from the center of the fiber and *d* denotes the diameter of the air core.

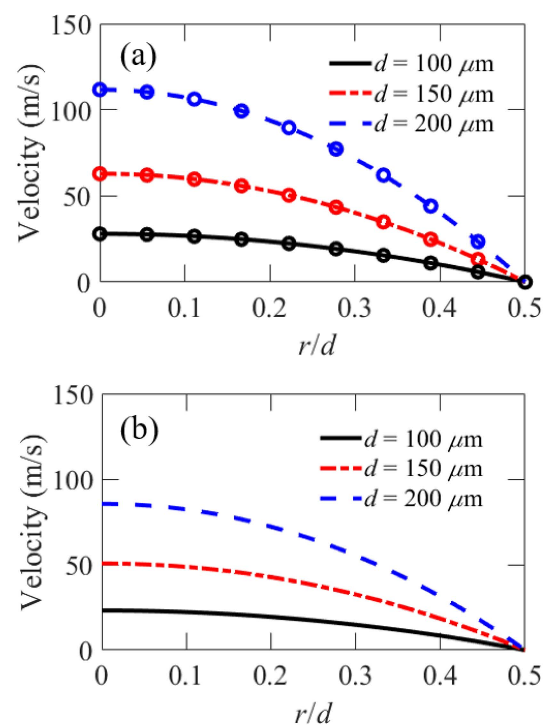

Fig. 2. Velocity profiles at the midpoint of the fiber as a function of the ratio of radial distance to the core diameter *r/d* for (a) the incompressible model and (b) the compressible model.

so we can take advantage of axial symmetry to reduce the problem to two dimensions, greatly reducing computational demands. This simple cylindrical shape corresponds to a straight fiber. When a fiber is bent, both the mode profile and the gas flow in the hollow core are altered, requiring three dimensional simulations. Fig. 1 shows a schematic illustration of the hollow core fiber. The parameter *r* denotes the radial distance from the center of the fiber and *d* denotes the diameter of the air core. Within the air core, the ratio *r/d* varies from 0 to 0.5. Hollow-core fiber lasers in the mid-IR wavelength range typically have core diameters on the order of 100 micrometers [15], [26], [33], [34], [35]. In this study, we vary the diameter from 100 to 200 μm. Experimental work has used hollow-core fiber with a length ranging from several tens of centimeters [29], [36] to tens of meters [27], [37]. We carried out our simulations using a fiber length of 0.5 m unless otherwise specified.

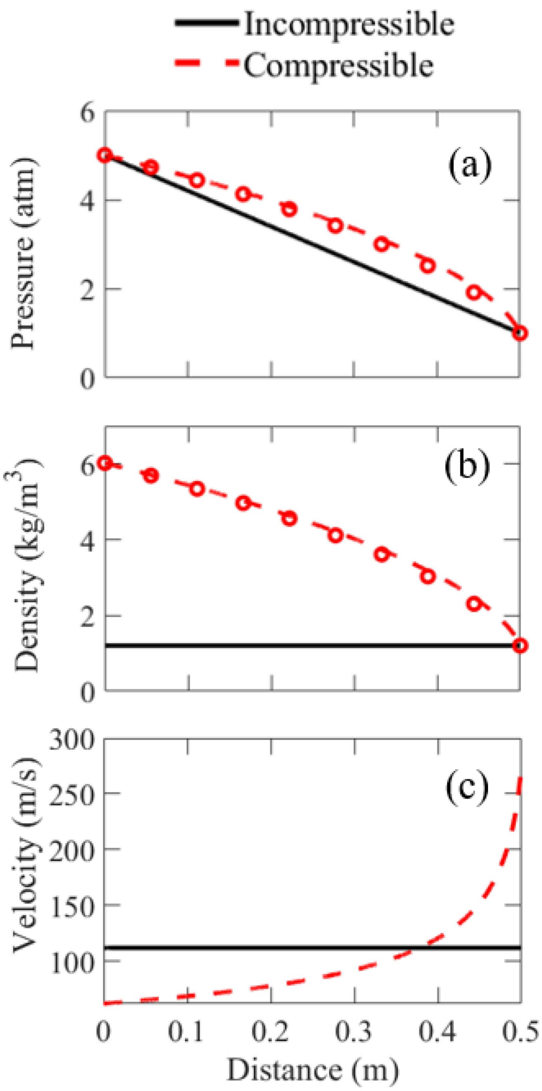

Fig. 3. (a) Pressure, (b) density, and (c) velocity profiles at the center of the fiber in the longitudinal direction for the incompressible model and the compressible model.

Fig. 2(a) and (b) illustrate the velocity profiles at the midpoint of the fiber as a function of the ratio of radial distance to the hollow-core diameter *r*/*d*. We use a no-slip wall boundary condition. We use air as a gas medium in our simulation. The density ρ of air is calculated based on the ideal gas law. For air, the molar mass *M* is 29 g/mol, the ideal gas constant *R* is 8.32 J/(mol-K), and the viscosity of air μ is 1.8 × 10^{-5} Pa · s in our simulation [38]. We find that velocity increases with increasing core diameter. We also see that the incompressible model produces velocities that are consistently higher than those produced by the compressible model at the midpoint of the fiber. The circles indicate the analytical solution of velocity profiles along transverse direction for the incompressible model [39] for different core diameters, which matches well with numerical solutions.

Fig. 3 shows the profiles for pressure, density, and velocity at the fiber center in the longitudinal direction. Fig. 3(a) shows the pressure distribution for both the incompressible and compressible models. In the incompressible model, there is a linear decline in pressure from an inlet value of 5 atm to an outlet pressure of 1 atm. The pressure for the compressible model remains consistently above that of the incompressible model along the fiber and is no longer linear. The red circles indicate the analytical solution for the pressure along the fiber length for the compressible model [40], [41]. Fig. 3(b) shows the density profiles. In the incompressible model, density is uniform along the fiber's longitudinal direction. In the compressible model, the density is a function of pressure, $\rho = pM/(RT)$, being larger where the pressure is higher. The red circles indicate the analytical solution for the density along the fiber length for the compressible model. Fig. 3(c) shows the velocity profiles. In the incompressible model, velocity remains constant, suggesting a rigid-body motion of the gas where fluid molecules exhibit no relative movement and maintain identical velocities. The analytical solution for the incompressible model [39] produces a velocity of 112 m/s, which matches well with the black line in Fig. 3(c). On the other hand, the compressible model produces an increasing velocity profile that reaches a maximum near the outlet. The gas velocity increases in the longitudinal direction due to the consistently higher pressure near the inlet compared to the outlet, driving the gas to increase its velocity as it moves along the hollow-core fiber. This study expands on prior work [24] and further illustrates that it is essential to use the compressible model. The results are consistent with prior work that studied the gas concentration and the gas filling time in hollow-core fibers [42]. The decision to use incompressible flow or compressible flow in modeling gas flow depends on several factors, including the Mach number of the flow, the desired level of accuracy, and the specific application [43], [44], [45], [46]. Since the compressible model offers a more realistic simulation of gas flow, which yields different results compared with the incompressible model, we use the compressible model in the remainder of this paper.

III. Gas Flow and Heat Transfer Coupled Model

Fiber lasers can deliver high output powers [3], [4], [5], [6], [9]. However, these high output powers can lead to excessive heat, which can impair laser performance or even damage the host fiber. It is a unique feature for hollow-core fibers that thermal mitigation can be achieved by using gas flow. In this section, we will focus on the heat transfer model in a steady-state solution. The heat transfer equation in steady-state is given by [30], [47], [48]

$$\rho C \mathbf{u} \cdot \nabla T = \kappa \nabla^2 T + Q, \quad (2)$$

where $\mathbf{u}$ is the fluid velocity, *T* is the temperature, ρ is the density, *C* is the heat capacity, κ is thermal conductivity, and *Q* is the heat density of heat source. Through the heat transfer equation, we can determine the temperature distribution due to the heat generated in the lasing process, as well as the gas flow.

We use a coupled model to study the gas flow and heat transfer simultaneously. At a higher temperature, the gas density decreases and viscosity increases, which affect the gas flow

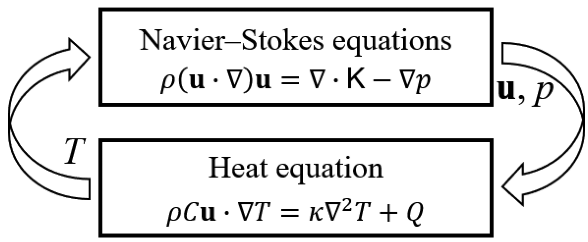

Fig. 4. Schematic illustration of the coupled model. The density ρ in the navier-stokes equations is updated based on the temperature T and pressure p in each iteration, $\rho = pM/(RT)$.

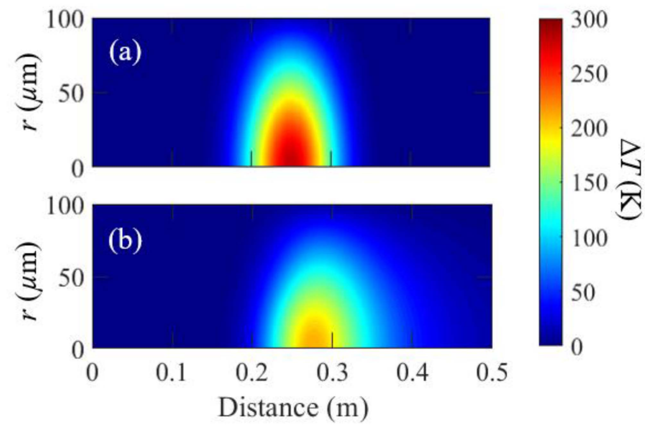

Fig. 5. Temperature increase ΔT from the ambient temperature (a) without and (b) with gas flow.

through the fiber. Simultaneously, the gas flow transports the heat in the longitudinal direction. Hence, in the coupled model, after we execute the gas flow model, the calculated values of gas velocity $\mathbf{u}$ and gas pressure p are passed to the heat transfer model as its initial conditions. The heat transfer model then determines the temperature, which is then passed back to the gas flow model to determine the gas density $\rho = pM/(RT)$ and viscosity μ, which is a function of temperature T. We then repeat this process iteratively until it converges. Fig. 4 shows a schematic illustration of the couped model. We use steady-state solutions in the gas flow model and heat transfer model to study the gas flow and heat transfer process.

We use COMSOL Multiphysics to find the solution of the heat equation. In the simulation, we model the hollow core filled with air and the glass cladding, as shown in Fig. 1. We model the heat transfer using a 2D axial symmetry. The diameter of the hollow core is 200 μm, which is surrounded by a glass layer. The fiber length is 0.5 m. In the appendix, we show the viscosity, heat capacity, and thermal conductivity for air as a function of temperature. The density of glass is 2203 kg/m^3. The thermal conductivity of glass is 1.38 W/m-K. The heat capacity of glass is 703 J/kg-K [49]. The temperature at the outer boundary of the glass cladding is set to the ambient temperature of 293 K. We assume that the heat source has a Gaussian distribution along the fiber's longitudinal direction, representing the heat generated in a gas-filled hollow-core fiber laser, which is consistent with the temperature profiles in the optical fiber amplifiers using solid core fibers [50], [51], [52]. We set the heat maximum at the center and full-width half-maximum (FWHM) equal to quarter of the fiber length [50], [51], [52]. We will later show that the results remain qualitatively similar regardless of where the longitudinal heat profile has its maximum. We also assume that the heat profile is Gaussian-distributed in the transverse direction, due to the light amplification gain of a fundamental mode [53]. We use an FWHM equal to half the core diameter, consistent with the ratio of fundamental mode to the fiber core [54]. We set the total heat power equal to 5 W after integrating over the whole fiber spatial domain. The temperature variation within the air core is significantly larger than within the glass cladding because the thermal conductivity in air is 70 times smaller than that in the glass. Although we include glass in our heat transfer model, our subsequent discussion will only show the results of the temperature distribution within the air core.

In this paper, we demonstrate that gas flow within hollow-core fibers can lead to significant temperature reduction. With a fixed input pressure and beam profile, the optical beam will reach a steady state in the optical fiber, leading to a fixed heat profile. Here we assume a fixed heat profile, varying the initial gas pressure, so that we can determine the thermal mitigation due to increased gas pressure. Future research will extend our model to dynamically couple gas flow, heat transfer, and laser gain dynamics.

IV. Simulation Results for Various Conditions

Fig. 5 shows the increase in relative temperature ΔT from the ambient temperature, which is assumed to equal 293 K. Without gas flow as shown in Fig. 5(a), the maximum temperature is located in the middle of the fiber at the peak of heat profile. With gas flow as shown in Fig. 5(b), the temperature peak shifts in the direction of the gas flow, and the maximum temperature also decreases at the same time.

Fig. 6(a) shows the temperature distribution in the longitudinal direction at the fiber center for differential pressure ΔP, which is defined as the difference in pressure between the two ends of the fiber. The temperature distribution profile broadens as ΔP increases, due to the air flow from the inlet to the outlet. Again, the shift results in an asymmetrical temperature distribution due to the air flow, deviating from the initial symmetrical profile with $\Delta P = 0$. A larger pressure difference leads to a larger shift of the peaks of the temperature curves and a lower maximum temperature. The maximum $\Delta P = 10$ atm can be readily available in the laboratory setting using a pressurized gas cylinder [55], [56]. Based on Fig. 6(a), we further plot the maximum temperature as a function of differential pressure, ΔP in Fig. 6(b). Due to the gas flow, the maximum ΔT decreases more than 20% from 273 K to 208 K, which demonstrates that the gas flow within the hollow core of the fiber enhances the heat dissipation.

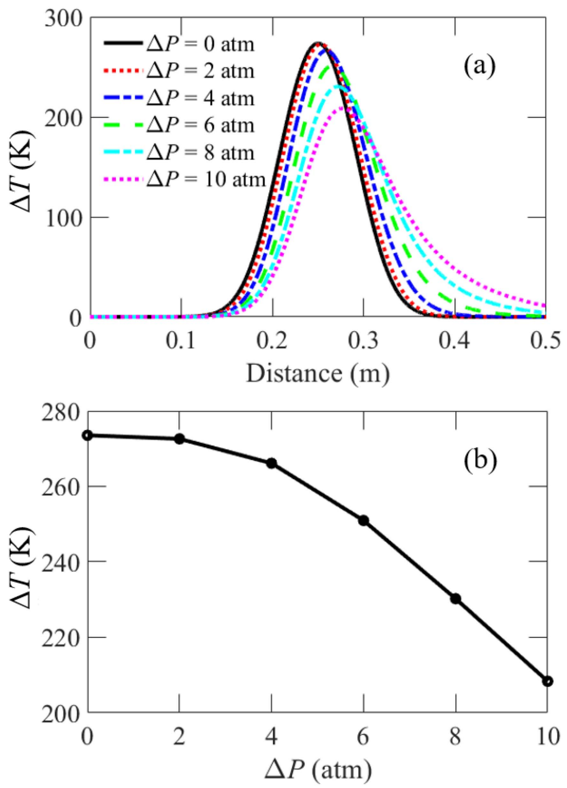

Fig. 6. (a) The temperature profile in the longitudinal direction in the center of the fiber as a function of distance as we vary ΔP. (b) The maximum ΔT as a function of ΔP. The fiber length is 0.5 m, and the core diameter is 200 μm.

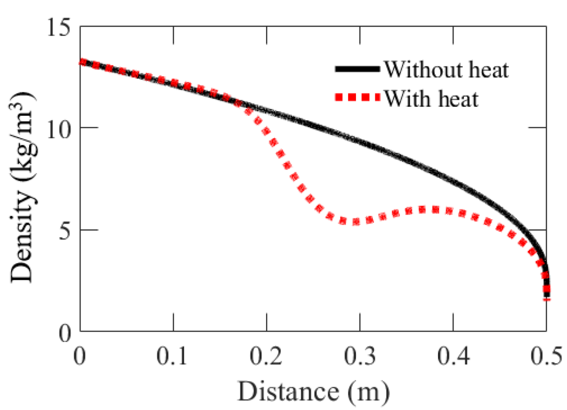

Fig. 7. Density profiles at the center of the fiber in the longitudinal direction with and without heat.

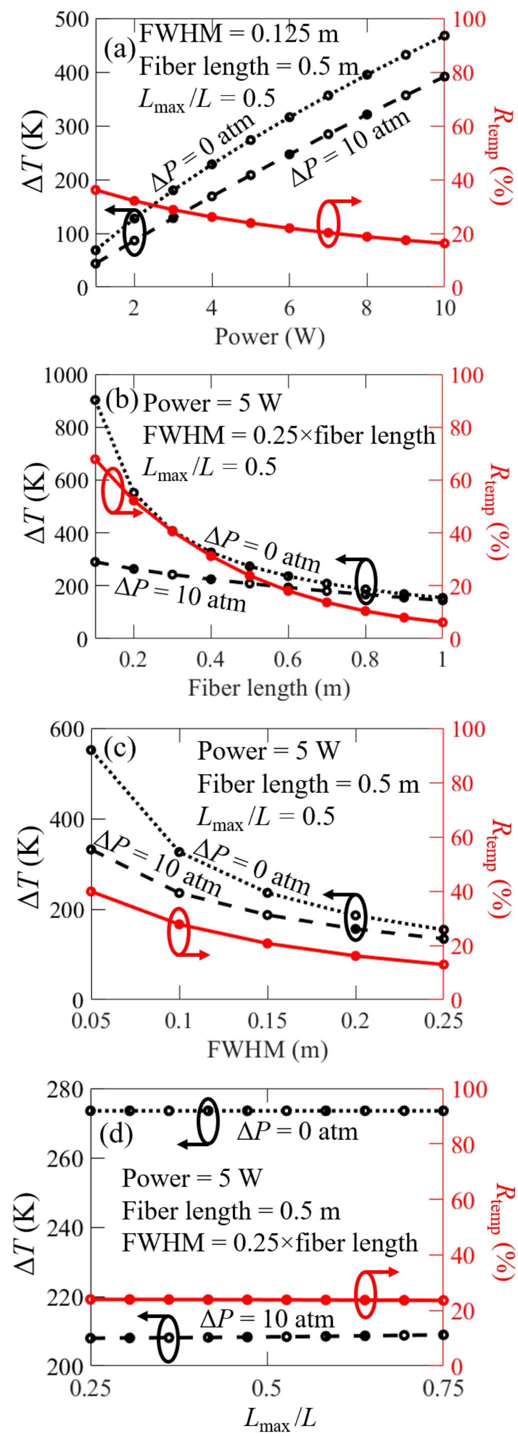

Fig. 8. The relative temperature change ΔT and relative temperature reduction, R_{temp}, at the center of the fiber as a function of (a) the heat power, (b) the fiber length, (c) the FWHM of the heat profile, and (d) $L_{\max}$ $/L$, the ratio of location at which the heat profile is maximum to the fiber length.

We further study the influence of temperature on the density in the coupled model. Fig. 7 shows the density at the center of the fiber with and without heat. We set $\Delta P = 10$ atm in the simulation. The curve without heat is obtained from the gas flow model only. The curve with heat is obtained from the coupled model. For the curve with heat, there is a dip at around a distance of 0.3 m, corresponding to the high temperature point in Fig. 6(a). The heat changes the density significantly.

In Fig. 8, we show the variation of the temperature change ΔT as we vary the heat power, fiber length, and FWHM of the heat profile, and the location at which the heat profile is maximum. We define relative temperature reduction, R_{temp}, using the following equation,

$$R_{\mathrm{temp}} = \frac{\Delta T_{\Delta P=0} - \Delta T_{\Delta P=10\ \mathrm{atm}}}{\Delta T_{\Delta P=0}} \times 100\%, \qquad (3)$$

where $\Delta T_{\Delta P=0}$ and $\Delta T_{\Delta P=10 \text{ atm}}$ are the relative temperature increase from the ambient temperature with $\Delta P = 0$ atm and $\Delta P = 10$ atm, respectively. Fig. 8(a) shows ΔT as a function of the heat power. The figure indicates that relative temperature reduction, R_{temp}, decreases from 40% to 20% with gas flow when heat power increases from 1 W to 10 W. Fig. 8(b) presents ΔT as a function of fiber length. This figure shows that the temperature reduction increases with shorter fiber, because the heat in the hollow core flows out more rapidly when the fiber length is short. Fig. 8(c) illustrates the ΔT as a function of the FWHM of the heat profile. When the heat is more concentrated, it leads to a more temperature reduction with gas flow. In Fig. 8(d), we show ΔT as a function of ratio of location, $L_{\max}$, at which the heat profile is maximum to the fiber length L. The location at which the heat profile is maximum does not have much impact on ΔT.

V. Conclusion

We theoretically model temperature mitigation in hollow-core fibers through gas flow. While the motivation for this study is the heat that is generated in high-power hollow-core optical fiber lasers, our results are independent of the heat source. We use a coupled model to study gas flow and heat transfer simultaneously in a hollow-core fiber. We first compare the results of using compressible and incompressible gas flow models using the Navier-Stokes equations. The significant difference between these two gas flow models demonstrates the importance of using a compressible model to study the gas flow in hollow-core fibers. Then we use the coupled model to study the impact of gas flow on the temperature change along the fiber in steady state. We varied the total heat power, the fiber length, the FWHM of the heat profile, the location at which the heat profile is maximum, and the input pressure. We found that the relative temperature reduction increases when the total heat power decreases, the fiber becomes shorter, and the heat profile becomes more localized, while the location of the heat maximum has little impact. When the input pressure is 10 atm with a heat power of 5 W, the relative temperature reduction is always significant and can be as high as 20%.

The results indicate that hollow-core fiber termination methods that leave the end of the fiber unsealed may have significant advantages for power scaling of gas-filled fiber lasers. These results are sufficiently promising to justify further research that examines the more complex fiber geometries that are typically used in hollow-core fiber lasers such as negative curvature fibers. These results also justify the study of the heat deposition that occurs in the gain medium as the laser light passes through the optical fiber and the gain medium is itself swept through the fiber due to the differential pressure.

Appendix A
Material Properties of Air

Fig. 9 shows the (a) thermal conductivity, (b) heat capacity, (c) viscosity of air at different ΔT [38], [57], [58], [59].

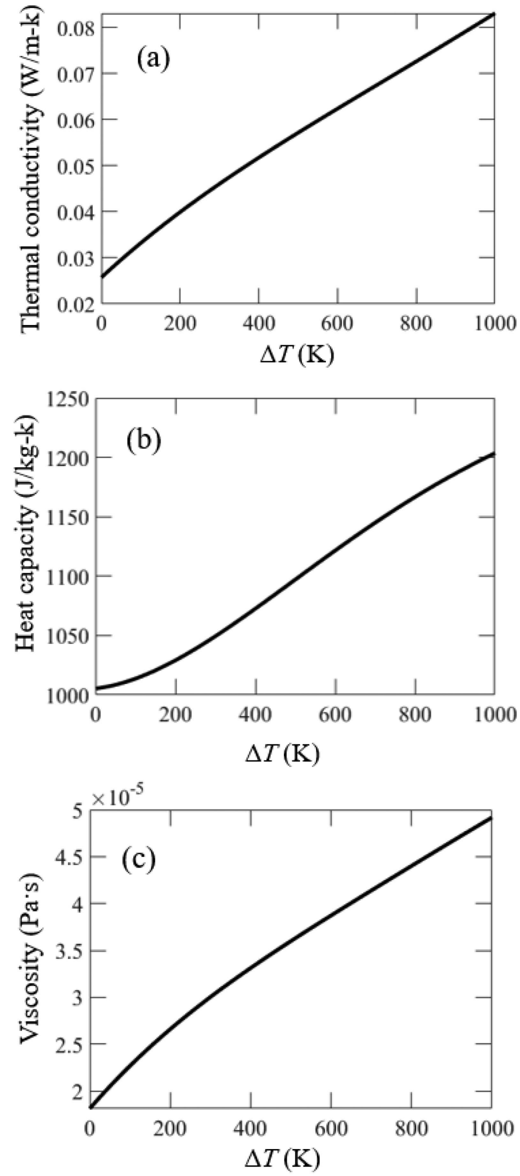

Fig. 9. (a) Thermal conductivity, (b) heat capacity, (c) viscosity of air.

Acknowledgment

The authors would like to express their appreciation to Dr. Nathaniel P. Lockwood for valuable discussions.

References

[1] B. E. Cherrington, *Gaseous Electronics and Gas Lasers*. Oxford, U.K.: Pergamon Press, 1979.

[2] M. Endo and R. F. Walter, *Gas Lasers*. New York, NY, USA: Taylor & Francis, 2007.

[3] Y. Kalisky and O. Kalisky, "The status of high-power lasers and their applications in the battlefield," *Opt. Eng.*, vol. 49, no. 9, Sep. 2010, Art. no. 091003, doi: 10.1117/1.3484954.

[4] A. V. V. Nampoothiri et al., "Hollow-core optical fiber gas lasers (HOFGLAS): A review," *Opt. Mater. Exp.*, vol. 2, no. 7, pp. 948–961, Jul. 2012, doi: 10.1364/Ome.2.000948.

[5] P. S. Russell, P. Holzer, W. Chang, A. Abdolvand, and J. C. Travers, "Hollow-core photonic crystal fibres for gas-based nonlinear optics," *Nature Photon.*, vol. 8, no. 4, pp. 278–286, Apr. 2014, doi: 10.1038/Nphoton.2013.312.

[6] F. Yang, F. Gyger, and L. Thevenaz, "Intense Brillouin amplification in gas using hollow-core waveguides," *Nature Photon.*, vol. 14, no. 11, pp. 700–708, Nov. 2020, doi: 10.1038/s41566-020-0676-z.
[7] P. Russell, "Photonic crystal fibers," *Science*, vol. 299, no. 5605, pp. 358–362, Jan. 2003, doi: 10.1126/science.1079280.
[8] R. A. Lane and T. J. Madden, "Numerical investigation of pulsed gas amplifiers operating in hollow-core optical fibers," *Opt. Exp.*, vol. 26, no. 12, pp. 15693–15704, Jun. 2018, doi: 10.1364/Oe.26.015693.
[9] J. C. Travers, W. K. Chang, J. Nold, N. Y. Joly, and P. S. J. Russell, "Ultrafast nonlinear optics in gas-filled hollow-core photonic crystal fibers," *J. Opt. Soc. Amer. B-Opt. Phys.*, vol. 28, no. 12, pp. A11–A26, Dec. 2011, doi: 10.1364/Josab.28.000a11.
[10] F. Benabid and P. J. Roberts, "Linear and nonlinear optical properties of hollow core photonic crystal fiber," *J. Modern Opt.*, vol. 58, no. 2, pp. 87–124, 2011, doi: 10.1080/09500340.2010.543706.
[11] A. R. Bhagwat and A. L. Gaeta, "Nonlinear optics in hollow-core photonic bandgap fibers," *Opt. Exp.*, vol. 16, no. 7, pp. 5035–5047, Mar. 2008, doi: 10.1364/Oe.16.005035.
[12] F. Yu and J. C. Knight, "Negative curvature hollow-core optical fiber," *IEEE J. Sel. Topics Quantum Electron.*, vol. 22, no. 2, Mar./Apr. 2016, Art. no. 4400610, doi: 10.1109/Jstqe.2015.2473140.
[13] C. L. Wei, R. J. Weiblen, C. R. Menyuk, and J. Hu, "Negative curvature fibers," *Adv. Opt. Photon.*, vol. 9, no. 3, pp. 504–561, Sep. 2017, doi: 10.1364/Aop.9.000504.
[14] B. Debord, F. Amrani, L. Vincetti, F. Gerome, and F. Benabid, "Hollow-core fiber technology: The rising of 'gas photonics'," *Fibers*, vol. 7, no. 2, Feb. 2019, Art. no. 16, doi: 10.3390/fib7020016.
[15] R. R. Gattass et al., "Infrared glass-based negative-curvature antiresonant fibers fabricated through extrusion," *Opt. Exp.*, vol. 24, no. 22, pp. 25697–25703, Oct. 2016, doi: 10.1364/Oe.24.025697.
[16] A. F. Kosolapov et al., "Demonstration of CO_2-laser power delivery through chalcogenide-glass fiber with negative-curvature hollow core," *Opt. Exp.*, vol. 19, no. 25, pp. 25723–25728, Dec. 2011, doi: 10.1364/Oe.19.025723.
[17] J. Henningsen and J. Hald, "Dynamics of gas flow in hollow core photonic bandgap fibers," *Appl. Opt.*, vol. 47, no. 15, pp. 2790–2797, May 2008, doi: 10.1364/Ao.47.002790.
[18] R. Wynne and B. Barabadi, "Gas-filling dynamics of a hollow-core photonic bandgap fiber for nonvacuum conditions," *Appl. Opt.*, vol. 54, no. 7, pp. 1751–1757, Mar. 2015, doi: 10.1364/Ao.54.001751.
[19] N. P. Lockwood, "Investigation of radio frequency discharges and Langmuir probe diagnostic methods in a fast flowing electronegative background gas," Ph.D. dissertation, Dept. Eng. Phys., AFIT, Dayton, OH, USA, 2007.
[20] I. Dicaire, J. C. Beugnot, and L. Thévenaz, "Analytical modeling of the gas-filling dynamics in photonic crystal fibers," *Appl. Opt.*, vol. 49, no. 24, pp. 4604–4609, Aug. 2010, doi: 10.1364/Ao.49.004604.
[21] B. M. Masum, S. M. Aminossadati, C. R. Leonardi, M. S. Kizil, and M. Amanzadeh, "Numerical analysis of gas diffusion in drilled hollow-core photonic crystal fibres," *Measurement*, vol. 127, pp. 283–291, Oct. 2018, doi: 10.1016/j.measurement.2018.05.106.
[22] B. M. Masum, S. M. Aminossadati, M. S. Kizil, and C. R. Leonardi, "Numerical and experimental investigations of pressure-driven gas flow in hollow-core photonic crystal fibers," *Appl. Opt.*, vol. 58, no. 4, pp. 963–972, Feb. 2019, doi: 10.1364/Ao.58.000963.
[23] B. M. Masum, S. M. Aminossadati, C. R. Leonardi, and M. S. Kizil, "Gas sensing with hollow-core photonic crystal fibres: A comparative study of mode analysis and gas flow performance," *Photon. Nanostructures-Fundam. Appl.*, vol. 41, Sep. 2020, Art. no. 100830, doi: 10.1016/j.photonics.2020.100830.
[24] W. Zhang, C. R. Menyuk, and J. Hu, "Modeling gas flow in hollow-core optical fibers," in *Proc. IEEE Photon. Conf.*, 2021, pp. 1–2, doi: 10.1109/Ipc48725.2021.9592930.
[25] N. Dadashzadeh et al., "Near diffraction-limited performance of an OPA pumped acetylene-filled hollow-core fiber laser in the mid-IR," *Opt. Exp.*, vol. 25, no. 12, pp. 13351–13358, Jun. 2017, doi: 10.1364/OE.25.013351.
[26] Z. F. Wang, W. Belardi, F. Yu, W. J. Wadsworth, and J. C. Knight, "Efficient diode-pumped mid-infrared emission from acetylene-filled hollow-core fiber," *Opt. Exp.*, vol. 22, no. 18, pp. 21872–21878, Sep. 2014, doi: 10.1364/Oe.22.021872.
[27] Z. Y. Zhou et al., "High-power tunable mid-infrared fiber gas laser source by acetylene-filled hollow-core fibers," *Opt. Exp.*, vol. 26, no. 15, pp. 19144–19153, Jul. 2018, doi: 10.1364/Oe.26.019144.
[28] W. Huang et al., "Fiber laser source of 8 W at 3.1 μm based on acetylene-filled hollow-core silica fibers," *Opt. Lett.*, vol. 47, no. 9, pp. 2354–2357, May 2022, doi: 10.1364/Ol.457265.
[29] F. B. A. Aghbolagh et al., "Mid IR hollow core fiber gas laser emitting at 4.6 μm," *Opt. Lett.*, vol. 44, no. 2, pp. 383–386, Jan. 2019, doi: 10.1364/Ol.44.000383.
[30] D. Anderson, J. C. Tannehill, R. H. Pletcher, R. Munipalli, and V. Shankar, *Computational Fluid Mechanics and Heat Transfer*, 4th ed. Boca Raton, FL, USA: CRC Press, 2020.
[31] G. Seregin, *Lecture Notes on Regularity Theory for the Navier-Stokes Equations*. Singapore: World Sci., 2014.
[32] L. D. Landau and E. M. Lifshitz, *Fluid Mechanics*. Reading, MA, USA: Addison-Wesley, 1968.
[33] F. Yu et al., "Attenuation limit of silica-based hollow-core fiber at mid-IR wavelengths," *APL Photon.*, vol. 4, no. 8, Aug. 2019, doi: 10.1063/1.5115328.
[34] A. Ventura et al., "Extruded tellurite antiresonant hollow core fiber for mid-IR operation," *Opt. Exp.*, vol. 28, no. 11, pp. 16542–16553, May 2020, doi: 10.1364/Oe.390517.
[35] A. Pryamikov, "Gas fiber lasers may represent a breakthrough in creating powerful radiation sources in the mid-IR," *Light: Sci. Appl.*, vol. 11, no. 1, Feb. 2022, doi: 10.1038/s41377-022-00728-5.
[36] A. V. V. Nampoothiri et al., "CW hollow-core optically pumped I fiber gas laser," *Opt. Lett.*, vol. 40, no. 4, pp. 605–608, Feb. 2015, doi: 10.1364/Ol.40.000605.
[37] Z. Zhou et al., "Towards high-power mid-IR light source tunable from 3.8 to 4.5 microm by HBr-filled hollow-core silica fibres," *Light Sci. Appl.*, vol. 11, no. 1, Jan. 2022, Art. no. 15, doi: 10.1038/s41377-021-00703-6.
[38] B. E. Poling, J. M. Prausnitz, and J. P. O'Connell, *The Properties of Gases and Liquids*, 5th ed. New York, NY, USA: McGraw Hill, 2000.
[39] B. R. Munson, A. P. Rothmayer, T. H. Okiishi, and W. W. Huebsch, *Fundamentals of Fluid Mechanics*. Hoboken, NJ, USA: Wiley, 2012.
[40] C. Markos, J. C. Travers, A. Abdolvand, B. J. Eggleton, and O. Bang, "Hybrid photonic-crystal fiber," *Rev. Modern Phys.*, vol. 89, no. 4, Nov. 2017, doi: 10.1103/RevModPhys.89.045003.
[41] T. W. Kelly et al., "Gas-induced differential refractive index enhanced guidance in hollow-core optical fibers," *Optica*, vol. 8, no. 6, pp. 916–920, Jun. 2021, doi: 10.1364/Optica.424224.
[42] P. Bojes et al., "Experimental and numerical analysis of gas flow in nodeless antiresonant hollow-core fibers for optimization of laser gas spectroscopy sensors," *Opt. Laser Technol.*, vol. 152, Aug. 2022, Art. no. 108157, doi: 10.1016/j.optlastec.2022.108157.
[43] F. White, *Fluid Mechanics*. New York, NY, USA: McGraw Hill, 2015.
[44] R. C. Dorf, *The Engineering Handbook*, (The Electrical Engineering Handbook). Boca Raton, FL, USA: CRC Press, 2004.
[45] M. Escudier, "Compressible pipe flow," in *Introduction to Engineering Fluid Mechanics*. London, U.K.: Oxford Univ. Press, 2017, pp. 330–361.
[46] C. Wong, T. Zoeller, D. R. Adkins, and J. Shadid, "Investigation of gas flow in long and narrow channels," in *Proc. ASME Fluids Eng. Division Summer Meeting*, 2000.
[47] A. Bejan and A. D. Kraus, *Heat Transfer Handbook*. Hoboken, NJ, USA: Wiley, 2003.
[48] F. P. Incropera and D. P. DeWitt, *Fundamentals of Heat and Mass Transfer*, 4th ed. Hoboken, NJ, USA: Wiley, 1996.
[49] D. R. Lide, *CRC Handbook of Chemistry and Physics*. Boca Raton, FL, USA: CRC Press, 2003.
[50] S. Naderi, I. Dajani, T. Madden, and C. Robin, "Investigations of modal instabilities in fiber amplifiers through detailed numerical simulations," *Opt. Exp.*, vol. 21, no. 13, pp. 16111–16129, Jul. 2013, doi: 10.1364/Oe.21.016111.
[51] C. R. Menyuk et al., "Accurate and efficient modeling of the transverse mode instability in high energy laser amplifiers," *Opt. Exp.*, vol. 29, no. 12, pp. 17746–17757, Jun. 2021, doi: 10.1364/Oe.426040.
[52] J. T. Young et al., "Tradeoff between the Brillouin and transverse mode instabilities in Yb-doped fiber amplifiers," *Opt. Exp.*, vol. 30, no. 22, pp. 40691–40703, Oct. 2022, doi: 10.1364/Oe.472829.
[53] K. Wisal, C. Chen, H. Cao, and A. D. Stone, "Theory of transverse mode instability in fiber amplifiers with multimode excitations," *APL Photon.*, vol. 9, no. 6, Jun. 2024.
[54] W. Shere, G. T. Jasion, E. N. Fokoua, and F. Poletti, "Understanding the impact of cladding modes in multi-mode hollow-core antiresonant fibres," *Opt. Fiber Technol.*, vol. 71, Jul. 2022, Art. no. 102919, doi: 10.1016/j.yofte.2022.102919.
[55] B. Davis, *Practice Safety and Common Sense When Handling Compressed Gas Cylinders*. Cleveland, OH, USA: EHS Today, 2009.

[56] R. Periasamy, F. L. Chen, D. S. Ensor, R. P. Donovan, and R. Denyszyn, "Particles in high-pressure cylinder gases," *J. Aerosol Sci.*, vol. 12, no. 3, pp. 762–776, 1990, doi: 10.1080/02786829008959390.

[57] P. Foteinopoulos and A. Papacharalampopoulos P. Stavropoulos, "On thermal modeling of additive manufacturing processes," *CIRP J. Manuf. Sci. Technol.*, vol. 20, pp. 66–83, 2018.

[58] N. Gerzhova, J. Côté, P. Blanchet, C. Dagenais, and S. Ménard, "A conceptual framework for modelling the thermal conductivity of dry green roof substrates," *Bioresources*, vol. 14, no. 4, pp. 8573–8599, Nov. 2019, doi: 10.15376/biores.14.4.8573-8599.

[59] "Air - dynamic and kinematic viscosity," [Online]. Available: https://www.engineeringtoolbox.com/air-absolute-kinematic-viscosity-d_601.html

Wei Zhang (Graduate Student Member, IEEE) received the B.S. degree in electrical engineering and the M.S. degree in optical engineering from University of Electronic Science and Technology of China, Chengdu, Sichuan, China, in 2013 and 2016, respectively. He also received the M.S. degree in software development from University of Technology Sydney, Sydney, NSW, Australia in 2019. He is currently pursuing the Ph.D. degree in electrical and computer engineering at Baylor University, Waco, TX, USA. His research interests include photonic crystal fibers, gas fibers, nonlinear optics, nanophotonics, surface plasmon, simulation, and modeling.

Ryan A. Lane received his B.S. in physics from the University of Central Arkansas in 2008 and his Ph.D. in physics from the University of North Texas in 2016. Following his doctoral work, he worked with the Air Force Research Laboratory Laser Division investigating laser sources as a National Research Council Postdoctoral Associate. Since then, he has worked with Laser Division in multiple roles including as the program manager for the Novel High Energy Laser Sources program. His current research interests include hollow-core fiber lasers, ionization in diode-pumped alkali lasers, and nonlinear optics in high-power fiber lasers.

Curtis R. Menyuk (Life Fellow, IEEE) was born in 1954. He received the B.S. and M.S. degrees from MIT in 1976 and the Ph.D. from UCLA in 1981. He has worked as a research associate at the University of Maryland, College Park and at Science Applications International Corporation in McLean, VA. In 1986 he became an Associate Professor in the Department of Electrical Engineering at the University of Maryland Baltimore County, and he was the founding member of this department. In 1993, he was promoted to Professor. He was on partial leave from UMBC from Fall, 1996 until Fall, 2002. From 1996−2001, he worked part-time for the Department of Defense, co-directing the Optical Networking program at the DoD Laboratory for Telecommunications Sciences in Adelphi, MD from 1999−2001. In 2001−2002, he was Chief Scientist at PhotonEx Corporation. In 2008−2009, he was a JILA Visiting Fellow at the University of Colorado. In 2015−2016, he was a Visiting Fellow at the Max-Planck Institute for the Physics of Light in Erlangen, Germany. For the last 35 years, his primary research area has been theoretical and computational studies of lasers, microresonators, nonlinear optics, and fiber optics. He has authored or co-authored more than 320 archival journal publications as well as numerous other publications and presentations, and he is a co-inventor of six patents. He has also edited three books. The equations and algorithms that he and his research group at UMBC have developed to model optical fiber systems, laser systems, and other resonator systems are used extensively in the telecommunications and photonics industry. He is a member of the Society for Industrial and Applied Mathematics and of SPIE. He is a fellow of the American Physical Society, the Optical Society of America, and the IEEE. He is the 1996−1999 UMBC Presidential Research Professor, the winner of the 2013 IEEE Photonics Society William Streifer Award, a 2015−2016 winner of the Humboldt Foundation Research Award, and the winner of the 2024 SPIE G. G. Stokes Award. He is currently serving as the director of the UMBC Center for Navigation, Time, and Frequency Studies.

Jonathan Hu (Senior Member, IEEE) received his Ph.D. degree from the University of Maryland, Baltimore County in 2008. From 2009 to 2011, he was a Research Associate with Princeton University. He is now a Professor in the Department of Electrical and Computer Engineering at Baylor University. He has many years of research experience in optical sciences and engineering with expertise in the areas of mid-IR supercontinuum generation, chalcogenide glass fibers, photonic crystal fibers, high-power fiber lasers, nonlinear optics, nanophotonics, 2D materials, and surface plasmons. He was recognized as a Baylor Outstanding Faculty for Scholarship in 2022. He also served as a Baylor Fellow in 2018.